

# High Space Efficiency Hybrid Nanogenerators for Effective Water Wave Energy Harvesting

Chuguo Zhang, Wei Yuan, Baofeng Zhang, Ou Yang, Yuebo Liu, Lixia He, Jie Wang,\*  
and Zhong Lin Wang

Water wave energy is a vital renewable-energy resource, but it is less developed due to the characteristics of water wave with low and varying frequency. Herein, a bifilar-pendulum coupled hybrid nanogenerator (BCHNG) module, which includes an electromagnetic generator (EMG), two piezoelectric nanogenerators (PENGs), and two multilayer-structured triboelectric nanogenerators (TENGs), is incorporated into a vessel-like platform for wave energy harvesting. The combination of the lightweight TENG and the heavy PENG and EMG can not only increase the ability of power take-off to capture water wave energy, but also improve the space utilization rate of BCHNG module and facilitate the design of the floating wave energy collecting device. Furthermore, the BCHNG module can harvest the kinetic energy and gravitational potential energy of the water wave at the same time, which benefits from the two degrees of swing freedom of the bifilar-pendulum. Importantly, thanks to the accurate geometric design and the reasonable utilization of space, the BCHNG module achieves a high peak power density of  $358.5 \text{ W m}^{-3}$ . The findings not only provide a novel method for the large-scale development of blue energy, but also offer an opportunity for the development of self-powered marine resources.

pollution-free, and renewable energy system is an important part for the sustainable development of human beings.<sup>[1]</sup> Based on the advantages of large reserves and wide distribution, water wave energy is regarded as one of the vital clean energy sources.<sup>[2]</sup> However, due to the low frequency of ocean wave, it is difficult to be efficiently collected only by traditional electromagnetic generators (EMG), which need a high frequency operating condition to effectively convert wave energy into electricity.<sup>[3]</sup> Therefore, complex and cumbersome gearboxes are used to improve the efficiency of wave energy collection in various of bulky EMG devices, which are installed on the seabed.<sup>[4–6]</sup> However, these design schemes have many disadvantages, such as, extremely strict technical requirements, complicated installation process, and unfavorable maintenance.<sup>[7–9]</sup> In addition, piezoelectric nanogenerators (PENG) have been widely studied as

## 1. Introduction

The harvesting of renewable and clean energy in the surrounding environment of our daily life to build a green,

another kind of mechanical energy collection technology, which is also considered to harvest water wave energy.<sup>[10,11]</sup> However, due to the brittleness of PENG with the piezoelectric ceramic and the small output performance made of organic materials, the application of PENG in water wave energy collection is still restricted until now.

C. Zhang, W. Yuan, B. Zhang, O. Yang, Y. Liu, L. He, J. Wang, Z. L. Wang  
Beijing Institute of Nanoenergy and Nanosystems  
Chinese Academy of Sciences  
Beijing 100083, P. R. China  
E-mail: wangjie@binn.cas.cn

C. Zhang, W. Yuan, B. Zhang, O. Yang, L. He, J. Wang, Z. L. Wang  
College of Nanoscience and Technology  
University of Chinese Academy of Sciences  
Beijing 100049, P. R. China

Y. Liu, J. Wang  
Center on Nanoenergy Research  
School of Physical Science and Technology  
Guangxi University  
Nanning 530004, P. R. China

Z. L. Wang  
School of Materials Science and Engineering  
Georgia Institute of Technology  
Atlanta, GA 30332, USA

 The ORCID identification number(s) for the author(s) of this article can be found under <https://doi.org/10.1002/adfm.202111775>.

DOI: 10.1002/adfm.202111775

Triboelectric nanogenerator (TENG), based on the triboelectrification and electrostatic induction,<sup>[12]</sup> has been developed to harvest mechanical energy in 2012. Taking the advantages of wide selection of materials, low cost and diversity of structural design,<sup>[13,14]</sup> it is widely applied in self-powered sensor, micro/nano energy, and high-voltage source.<sup>[15–25]</sup> In addition, combining the characteristics of TENG's lightweight and high efficiency at low frequency with the characteristics of low frequency motion of water wave, the TENG has been considered to be one of the most potential technologies for wave energy harvesting, which can be achieved by constructing floating wave energy harvesting devices.<sup>[3,26]</sup> Therefore, all kinds of structural TENG, such as rolling spheres and spring-assisted structures,<sup>[27,28]</sup> have been designed for wave energy collection by the connective networks of TENGs.<sup>[29–34]</sup> However, these TENG can only harvest the kinetic energy of ocean wave in the propagative direction or the gravitational potential energy of ocean wave in the vertical direction,<sup>[34]</sup> which can hardly effectively harvest the kinetic energy and gravitational potential energy of ocean wave

at the same time. In our previous work, the vessel-like platform is proposed to harvest the ocean wave by integrating the bifilar-pendulum-assisted multilayer-structured triboelectric nanogenerators (M-TENG) modules.<sup>[26]</sup> A high peak power density was achieved in that work and the vessel platform had the ability to eliminate the influence of marine environment on the output performance of TENG.<sup>[35]</sup> However, it remains a vital research direction to improve the power density of ocean wave energy harvesting device by using TENG as much as possible through reasonable space utilization.<sup>[37,38]</sup>

In this work, we present a wave energy collection device by using a vessel platform to integrate bifilar-pendulum coupled hybrid nanogenerator (BCHNG) modules, which consists of an EMG, two PENGs, and two M-TENGs. Combined with the inevitable demand of M-TENG's with the power take-off (PTO) and the heavy characteristics of EMG and PENG, the coil of EMG and PENGs are designed as the PTO of M-TENG by the reasonable geometric structure design, which reasonably optimizes the space utilization rate of the device. As BCHNG modules are incorporated into a vessel, the stable environment inside the hull platform can facilitate the maintenance and long-term stable operation of the device. Thus, the installation and packaging process of the wave energy collecting device can be simplified by this design. Benefiting from the seesaw motion of vessel and the swing of bifilar-pendulum, the BCHNG can harvest the low-frequency ocean-wave with kinetic energy and gravitational potential energy, simultaneously. According to the reasonable utilization of space, the designed BCHNG module achieves a higher peak power density of  $358.5 \text{ W m}^{-3}$ . Our findings not only provide a new method to harvest the kinetic energy and gravitational potential energy of water wave at the same time, but also facilitate the application of blue energy to realize the self-powered marine sensing and seawater resources extraction in the future.

## 2. Results and Discussion

### 2.1. Structural Design and Working Mechanism

Based on our previous work, the proposed vessel platform can provide a stable working environment and reduce operating costs for ocean-wave energy collection device.<sup>[26]</sup> In addition, the vessel also can assist ocean-wave energy collection device to realize the multifunctionality of blue energy in situ. Therefore, the BCHNG modules are incorporated into a vessel to harvest wave energy (Figure 1a). The BCHNG module mainly includes an EMG located in the center, two PENGs, and M-TENG on both sides and a bifilar-pendulum structure (Figure 1b). The detailed structure of BCHNG module and three kinds of generators are depicted in Figure 1c and Figure S1, Supporting Information, where the wedge-shaped copper pendulum cone of bifilar-pendulum is wound with coils and then attached by two PENGs. Thus, the EMG is composed by a pair of trapezoidal magnets on the both sides and the wedge-shaped coil in the middle. The PENG is fabricated by a copper electrode in the middle, two lead lanthanum zirconate titanate (PZT) ceramic sheets on both sides, and two silver electrodes on the outside. The M-TENG is fabricated by a zigzag Kapton substrate,

copper electrodes, thin foams, and fluorinated ethylene propylene films (FEP,  $30 \mu\text{m}$ ). Figure 1d depicts the power transfer chain of vessel with integrated BCHNG modules for harvesting ocean-wave energy. It is obvious that the vessel is used as the primary interface to intercept the power of wave, the bifilar-pendulum is served as the PTO to capture the intercepted power of vessel, and the three kinds of generators are utilized to deliver the captured power of PTO into electric energy. The bifilar-pendulum cone is fabricated by using the heavy characteristics of PENG and the coil of EMG as the PTO and the light-weight characteristics of TENG is used to balance the weight of bifilar-pendulum cone, this design can not only increase the ability of PTO to capture water wave energy, but also add the space utilization-rate of BCHNG module and facilitate the design of floating wave energy collecting device. Besides, the good operation of BCHNG module is realized by the precise geometric design of BCHNG module (Figure S2 and Note S1, Supporting Information). To improve the output performance of M-TENG, a FEP film with micro/nano-structured surface and the foam as buffer layer are adopted to enhance the contact intimacy (Figure S3, Supporting Information).<sup>[39,40]</sup> Meanwhile, the foam as buffer layer can also prevent the piezoelectric ceramics from severe deformation to ensure the long-term stability of PENG. The near-offshore ocean-wave energy with unidirectional propagation mainly consists of the kinetic energy of seawater in the direction of propagation and the gravitational potential energy of seawater in the vertical direction (Figure S4, Supporting Information). Since the bifilar-pendulum can capture both the kinetic energy of water wave by horizontal inertia force and the gravitational potential energy of water wave by vertical gravity (Figure S5, Supporting Information), the BCHNG module can realize the efficient collection of the two kinds of mechanical energy of the waves in the near-offshore. Furthermore, in order to effectively harvest full frequency wave energy, the BCHNG modules with different natural motion frequencies can be designed by adjusting the line length of the bifilar-pendulum, and then different natural frequency BCHNG modules in the vessel can be designed according to the frequency distribution of the waves in a specific sea area to make full use of the resonance effect (Figure S6 and Note S2, Supporting Information). The motion module of the vessel with incorporated BCHNG modules in near-offshore ocean-waves is schematically illustrated in Figure S7, Supporting Information. Under the driving of ocean-waves, the vessel with incorporated BCHNG modules will generate a seesaw motion and the bifilar-pendulum will produce the corresponding swing at the same time. Meanwhile, the pendulum cone of bifilar-pendulum will continuously drive the coil of EMG to cut magnetic induction line, the piezoelectric ceramic of PENG to occur polarization induction effect, and the dielectric materials and electrodes of M-TENG to generate triboelectrification and electrostatic induction. Thus, the BCHNG modules transform the ocean-wave energy to the corresponding electric energy effectively. In summary, compared with the previous research work,<sup>[26]</sup> this work has the following advancements: 1) the bifilar-pendulum cone is fabricated by using the heavy characteristics of PENG and the coil of EMG as the PTO can increase the ability of PTO to capture water wave energy; 2) the bifilar-pendulum cone fabricated by the coil of EMG and PENG can significantly improve the space efficiency of water

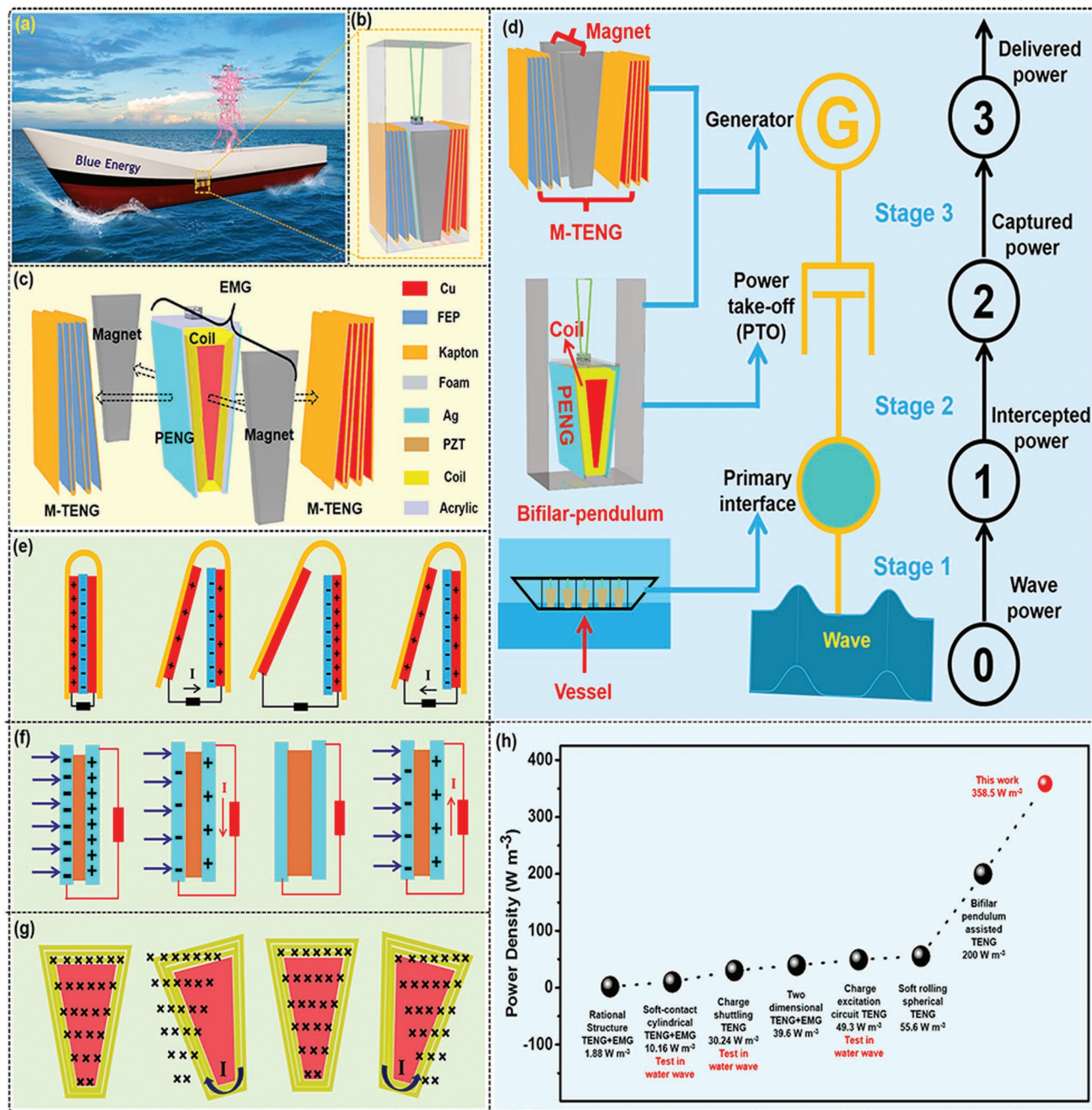


**Figure 1.** Structural design and working mechanism of the vessel with incorporated BCHNG modules. a) Device configuration of the Vessel with incorporated BCHNG modules. b) Schematic representation of enlarged structure for the BCHNG module. c) Structural components for BCHNG with three kinds of generators. d) The power transfer chain of the Vessel with incorporated BCHNG modules for harvesting ocean-wave energy. The working principles of e) TENG unit, f) PENG unit, and g) EMG. h) State-of-the-art performance of the device structure with the wave energy harvesting.

wave energy harvesting device and efficiently avoid the serious space waste caused by the bifilar-pendulum cone composed of copper blocks in the relative research work; 3) benefiting from the hybrid EMG and PENG, the output performance of water wave energy harvesting device is greatly boosted; 4) according to ingenious structural design, the stability of the whole device is greatly enhanced by the full application of three generators with the respective characteristics. The working mechanism

of BCHNG with three kinds of generators is displayed in the Figures 1e–g, respectively. For the M-TENG, after the iterative contact-separation process between the left Cu electrode and the right dielectric material (FEP film), the FEP film generates triboelectric negative charges and the Cu electrode produces triboelectric positive charge according to the triboelectric sequence. As the contact-separation between the left electrode and the right dielectric material FEP film, the alternative

current in the circuit will generate due to the electrostatic induction effect (Figure 1e). For the PENG, when the pendulum cone of bifilar-pendulum strike PENG parts under the driving of ocean-waves, the PZT sheet will produce internal strain and the two electrodes will generate opposite piezoelectric potential and then an alternating current is generated in the external circuit (Figure 1f). For the EMG, according to electromagnetic induction law, since the coil cuts the magnetic induction line of magnet, the current in a coil is induced by a changing magnetic field (Figure 1g). When the coil swings from right to middle, the current of the coil flows clockwise. As the coil backs from left to middle, the current of the coil flows counterclockwise.

Benefitting from the reasonable utilization of space, the peak power density of  $358.5 \text{ W m}^{-3}$  is achieved by the BCHNG modules in the seesaw test. For the development of wave energy harvesting, the corresponding landmark works are summarized in Figure 1h. First, the spring-assisted TENG achieves the peak power density of  $1.88 \text{ W m}^{-3}$ , the soft-contact cylindrical TENG coupling EMG realizes the output performance of  $10.16 \text{ W m}^{-3}$  in the water test,<sup>[36,41]</sup> and the charge shuttling TENG obtains the value of  $30.24 \text{ W m}^{-3}$  in the water test.<sup>[42]</sup> Then, the value is improved to 39.6, 49.3, and  $55.6 \text{ W m}^{-3}$  by the new structure of 2D TENG coupling EMG,<sup>[43]</sup> charge excitation circuit TENG,<sup>[28]</sup> and soft rolling spherical TENG.<sup>[27]</sup> Furthermore, based on soft material, thin dielectric materials with micro/nano surface, and multilayered structure, the bifilar-pendulum-assisted TENG<sup>[26]</sup> reaches  $200 \text{ W m}^{-3}$ . Therefore, compared to the above landmark works, this work is a vital milestone for the development of blue energy.

## 2.2. The Output Performances of BCHNG Module at Horizontal Motion

As well as we know, the ocean waves contain abundant kinetic energy in the direction of propagation. In order to research the collection of ocean-wave kinetic energy by BCHNG module, a linear motor is utilized to simulate the operative module of BCHNG module under the driving of ocean-wave kinetic energy. The working mechanism of one cycle is shown in Figure 2a. As the linear motor moves to the left state, the bifilar-pendulum will move to the right side and strike the right board due to the inertia, which will make the dielectric layers of left M-TENG to separate with the left electrode and generate the alternative current between two Cu electrodes of M-TENG unit due to electrostatic induction. Meanwhile, the dielectric layers of right M-TENG contact with the right electrode generating the triboelectrification phenomenon on the surface of contacting materials. At the same time, the bifilar-pendulum will drive the PENG to strike the right board and EMG to reduce the magnetic induction line through the coil (Figure 2a[i]). When the bifilar-pendulum comes to middle state, it makes all the dielectric layers of M-TENG separate with all the electrodes and increases the magnetic induction line through the coil (Figure 2a[ii]). Since linear motor moves to the right state, the BCHNG module will generate a state opposite to the left state. Meanwhile, the left PENG will strike the board and the magnetic induction line of the coil will decrease (Figure 2a[iii]). When the amplitude of linear motor with reciprocating motion

is fixed to 60 mm, the acceleration and deceleration of the reciprocating motion are set at 1.0, 3.0, and  $5.0 \text{ m s}^{-2}$ , respectively. The output performances of BCHNG are shown in Figure 2b–g. The open-circuit voltages of M-TENG, PENG, and EMG increase from 400 to 600 V, 0.1 to 12 V, and 0.3 to 1.2 V with the acceleration increasing from 1.0 to  $5.0 \text{ m s}^{-2}$ , respectively. The short-circuit currents of M-TENG, PENG, and EMG increase from 0.02 to 0.27 mA, 0.1 to 2 mA, and 0.3 to 3.5 mA, with the acceleration increasing from 1.0 to  $5.0 \text{ m s}^{-2}$ , respectively. These experimental results also fully demonstrate the characteristic of TENG with high voltage and low current and the feature of EMG with low voltage and high current. Figure S8, Supporting Information, shows the transferred charges of M-TENG and PENG under the same test conditions; they increase with the acceleration from  $0.5 \mu\text{C}$  at  $1.0 \text{ m s}^{-2}$  to  $1.5 \mu\text{C}$  at  $5.0 \text{ m s}^{-2}$  and  $0.1 \mu\text{C}$  at  $1.0 \text{ m s}^{-2}$  to  $5.3 \mu\text{C}$  at  $5.0 \text{ m s}^{-2}$ , respectively. The peak power of BCHNG module with three kinds of generators driven by the different acceleration of linear motor are illustrated in Figure 2h–j. At the acceleration of  $5.0 \text{ m s}^{-2}$ , the peak power of M-TENG is 15 mW with the external loading resistance of 500 k $\Omega$ , the peak power of PENG is 7 mW with the external loading resistance of 2 k $\Omega$  and the peak power of EMG is 2 mW with the external loading resistance of 400  $\Omega$ , respectively. This experimental results also fully demonstrate the characteristic of TENG with high matching resistance and the feature of EMG with low internal resistance. According to the excellent output performance of BCHNG module in the linear motor, it displays a good performance for the collection of ocean-wave kinetic energy in the direction of propagation. In addition, Figure S9, Supporting Information, shows the long-term stability of three components generator with the 250 000 operation cycles. Although stability of M-TENG is lower than that of PENG and EMG, the BCHNG module can maintain about 80% electric output after 250 000 operation cycles (Figure S10 and Note S3, Supporting Information). This result indicates that the BCHNG module shows the remarkable long-term durability. In view of weak stability of M-TENG, this question can be solved by charge excitation technique to further improve the durability of the BCHNG module.<sup>[44,45]</sup>

## 2.3. The Output Performances of BCHNG Module at Vertical Motion

In addition to the kinetic energy contained in the propagation direction of sea water, water waves also contain huge gravitational potential energy in the vertical direction, which can drive a 10 000-ton ship to produce severe jolts. Based on the geometric and mathematical relationship between the position change of the center of gravity in the vertical direction and the rotation angle in the swing process of the seesaw, we use a seesaw to study the BCHNG module for harvesting the gravitational potential energy of ocean-wave in the vertical direction. It not only can provide the various precise parameters of motion for BCHNG module, but also can well simulate the motion mode of vessel with incorporated BCHNG modules in ocean waves. Working mechanism of the BCHNG module driven by seesaw is depicted in Figure 3a. Since the BCHNG module arrives at the left tilting state, the bifilar-pendulum

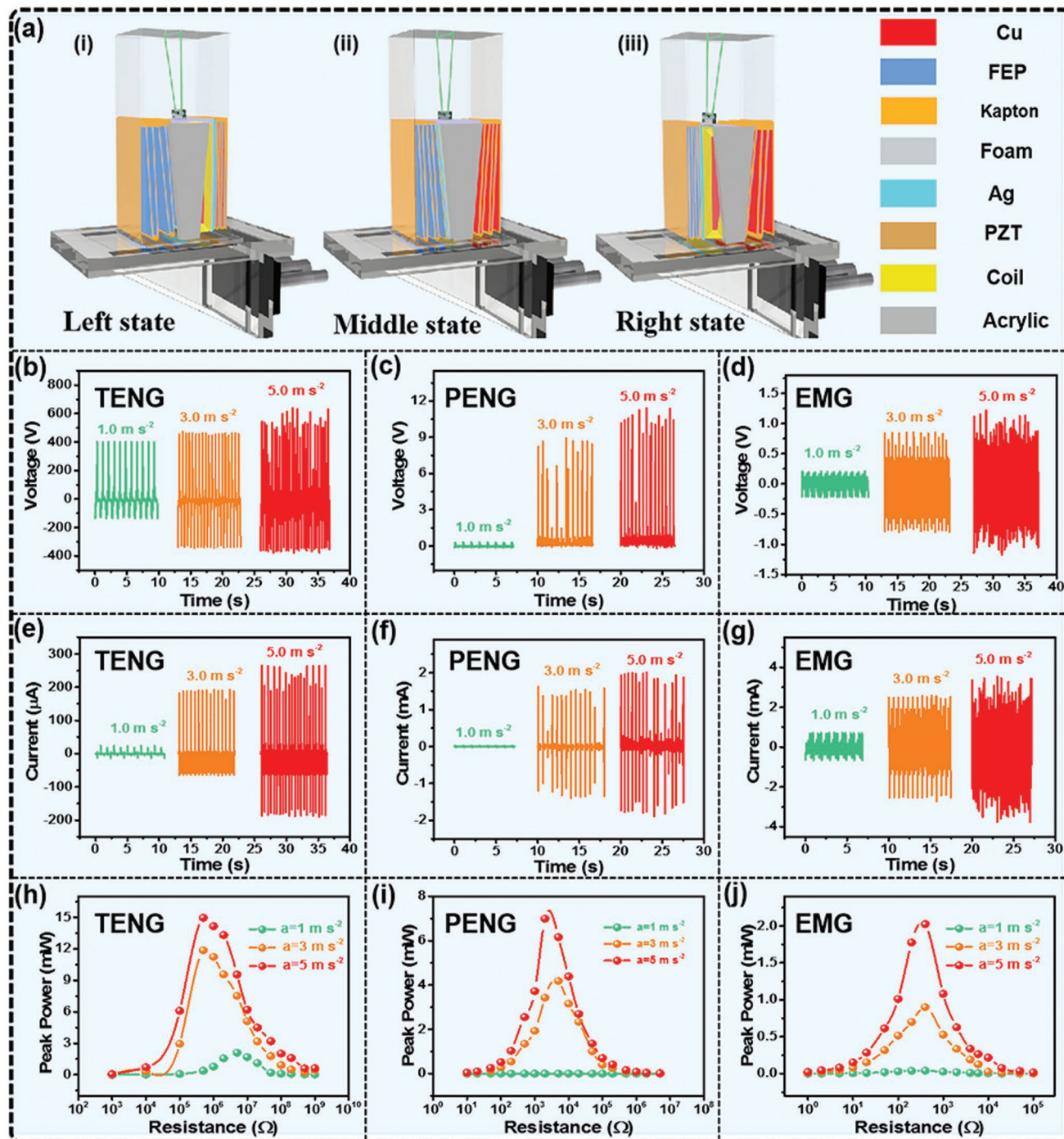


**Figure 2.** Output performance of the BCHNG module at horizontal motion. a) Operating mechanism of the BCHNG module driven by linear motor. The open-circuit voltage of b) M-TENG, c) PENG, and d) EMG with the various acceleration of linear motor. The short-circuit current of e) M-TENG, f) PENG, and g) EMG with the various acceleration of linear motor. The peak power of h) M-TENG, i) PENG, and j) EMG with the various acceleration of linear motor.

swings to the left board, resulting in the FEP films of left M-TENG contacting with the Cu electrodes and generating triboelectrification in between. Simultaneously, the FEP films of right M-TENG separating with the Cu electrodes and occurring the corresponding current between the two Cu electrodes of M-TENG unit. Meanwhile, the coil of EMG cuts the magnetic

sensing line from right to left and the left PENG strikes the left board (Figure 3a[i]). As the module comes to the medial equilibrium state, the FEP films of two M-TENGs on both sides will separate with the Cu electrodes together. Synchronously, the magnetic induction line through the coil will reach the maximum and the two PENGs will be back to the equilibrium

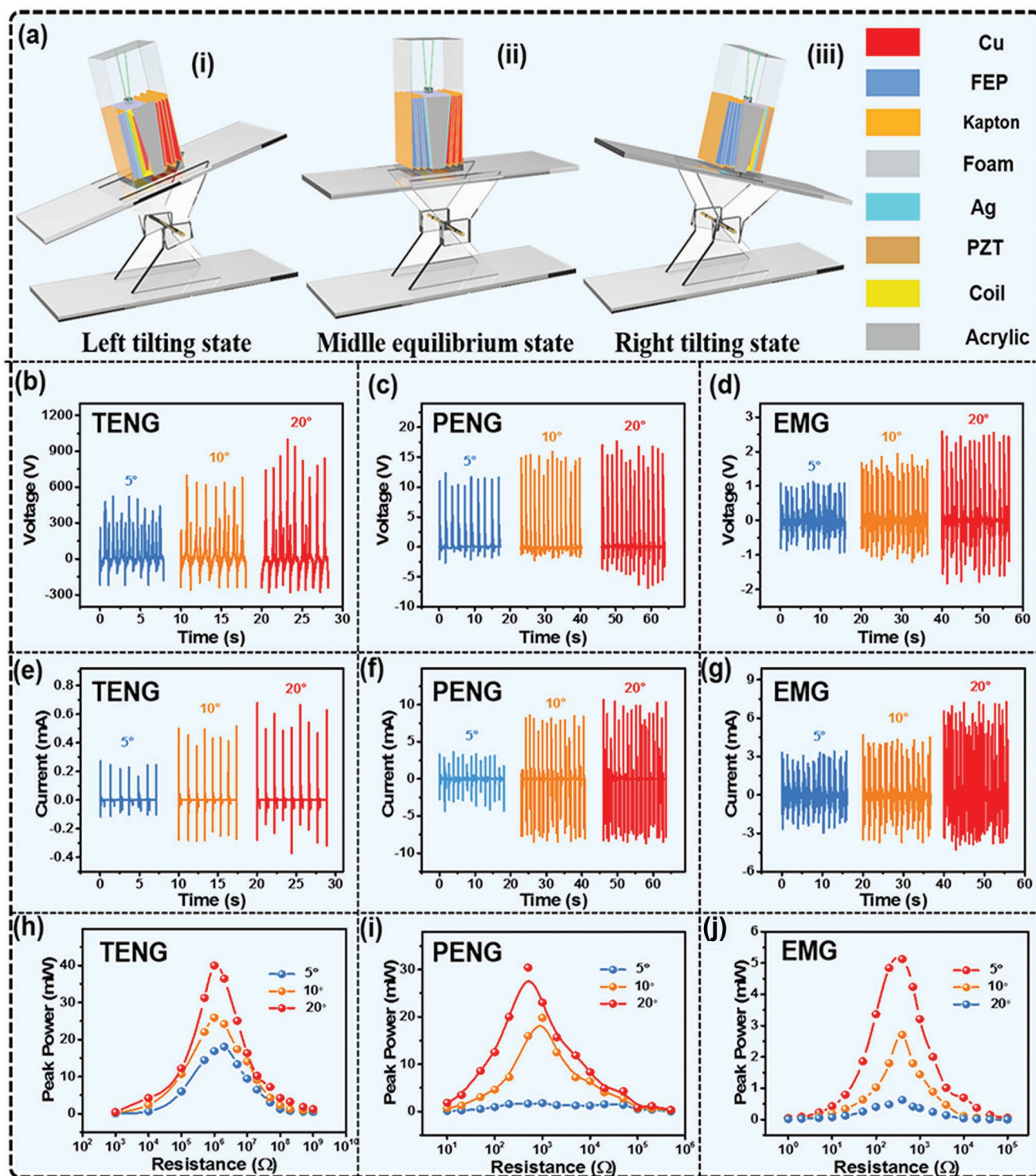


**Figure 3.** Output performance of the BCHNG at vertical motion. a) Working mechanism of the BCHNG module driven by seesaw. The open-circuit voltage of b) M-TENG, c) PENG, and d) EMG under the different angles of seesaw. The short-circuit currents of e) M-TENG, f) PENG, and g) EMG under the different angles of seesaw. The peak power curve of h) M-TENG, i) PENG, and j) EMG under the different angles of seesaw.

state (Figure 3a[ii]). Once the BCHNG module swings to the right tilting state, the BCHNG module will display a state opposed with the left tilting state (Figure 3a[iii]). The open-circuit voltage of M-TENG, PENG, and EMG under the

different rotation angles of seesaw are depicted in Figure 3b–d, respectively. The open-circuit voltages of M-TENG, PENG, and EMG increase from 500 to 900 V, 11 to 17 V, and 1 to 2.5 V with the rotation angle of seesaw from 5° to 20°, respectively.

Correspondingly, the short-circuit currents of M-TENG, PENG, and EMG increases from 0.3 to 0.7 mA, 3.4 to 10.6 mA, and 3 to 7 mA, respectively (Figure 3e–g). Under the same test conditions, the correlational transferred charges of M-TENG and PENG are presented in Figure S11, Supporting Information, and the transferred charges of M-TENG increase with the rotation angle of seesaw from 1.5  $\mu\text{C}$  at the  $5^\circ$  to 2.2  $\mu\text{C}$  at the  $20^\circ$  and the values of PENG increase with from 5.5 to 11  $\mu\text{C}$ . It is worth noting that the maximum surface charge density of M-TENG with 163  $\mu\text{C m}^{-2}$  is obtained even the contacted-area of M-TENG up to 135  $\text{cm}^2$ , which is almost three times as high as that of traditional TENG with the characteristic of large contact-area.<sup>[46]</sup> The first reason is that the thin of FEP film with the micro/nano surface structure can hold a high surface charge density (Figure S12, Supporting Information). The second reason is that the soft foam and the geometry structure design can help to improve the contact intimacy and triboelectric efficiency of FEP film. Meanwhile, the peak power curves of three kinds of generators with different external loading-resistance are presented in Figure 3h–k, the related peak power of three kinds of generator gradually increase with the rotation angle of seesaw. At the rotation angle of  $20^\circ$ , the M-TENG achieves the peak power of 39.2 mW at a matched load-resistance of 1  $\text{M}\Omega$ , the PENG realizes the peak power of 30 mW at a matched load-resistance of 700  $\Omega$ , and the EMG obtains the peak power of 2.5 mW at a matched load-resistance of 500  $\Omega$ , respectively. Therefore, the BCHNG module will achieve the peak power density of about 358.5  $\text{W m}^{-3}$ , which is composed of the M-TENG of 196  $\text{W m}^{-3}$ , the EMG of 12.5  $\text{W m}^{-3}$ , and the PENG of 150  $\text{W m}^{-3}$ , respectively. Compared with some previous classical research work for water wave energy collection, it is obvious to find that the BCHNG module can achieve higher power density output even under unfavorable driving conditions (Table S1). This result indicates that the BCHNG module can harvest large wave energy as well as collect water wave energy composed of small ripples.<sup>[27,35,36,47,48]</sup> In addition, it is obvious that the output performance of the module in the vertical direction is significantly higher than its test performance in the horizontal direction. The reason is that the relatively larger gravity, compared with the inertial force, can make the coil of EMG obtain a faster change rate and it also make M-TENG and PENG generate the more efficient uniform contact (Figure S13, Supporting Information). Figure S14, Supporting Information, shows that the average power of M-TENG is 1.14 mW at an external load-resistance of 20  $\text{M}\Omega$ , the average power of PENG is 0.98 mW at an external load-resistance of 2000  $\Omega$ , and the average power of EMG is the 0.26 mW at an external load-resistance of 1000  $\Omega$ , respectively (Note S4, Supporting Information). Therefore, the BCHNG module will realize the average power density of about 11.9  $\text{W m}^{-3}$ , which is composed of the M-TENG of 5.7  $\text{W m}^{-3}$ , the PENG of 4.9  $\text{W m}^{-3}$ , and the EMG of 1.3  $\text{W m}^{-3}$ , respectively. The contribution of the three generators for the average power of BCHNG module is 47.9% of the M-TENG, 41.2% of the PENG, and 10.9% of the EMG (Figure S15, Supporting Information) and the output performance of the BCHNG module can be further improved by the optimization of the number of units in M-TENG, the number of coils in EMG, the magnetic field strength of the magnet, and the thickness of ceramic plates in PENG. The high power density M-TENG results from the high surface charge density,

the good geometry structure design, and space utilization efficiency from multilayered-structure of TENG. Importantly, the BCHNG module can simultaneously harvest the kinetic energy and gravitational potential energy of ocean wave, which is beneficial from the swing of bifilar-pendulum.

#### 2.4. Output Performance and Applications of BCHNG in Water Wave

In order to better demonstrate the BCHNG module for harvesting ocean-wave energy, a boat with incorporated BCHNG module is installed in a water tank, which can simulate the motion of ocean-waves by the generated water waves (Figure 4a). Figure S16, Supporting Information, displays the photos of the fabricated BCHNG module. As demonstrated in Figure 4b and Movie S1, Supporting Information, the incorporated BCHNG module in the boat operating in simulating water waves can real-time drive a hygrothermograph (power: 60  $\mu\text{W}$  and screen size: 6.5  $\text{cm} \times 6 \text{ cm}$ ). The related circuit diagram is depicted in Figure 4c and the energy storage device is composed of two 100  $\mu\text{F}$  capacitors in series. In addition, the integrated BCHNG modules in the boat working in simulating waves can harvest water wave energy to store energy in the energy storage device (three 3.3 mF capacitors in parallels) and then drive a water quality detector (Movie S2 and Figure S17, Supporting Information). In the above process, every generator is connected with a rectifier bridge before linking with energy storage device to prevent the output counteraction due to the asynchronous motions. In the future, a vessel that integrates more BCHNG modules for water wave energy collection will be able to detect temperature, humidity, water quality in situ, and even drive a wireless signal transmission device to send the related data back to land for building a smart Marine Internet of Things network. Meanwhile, the corresponding peak power of incorporated BCHNG module in boat in simulating water waves is displayed in Figure 4d; the highest power of M-TENG, PENG, and EMG are 3.1, 2.9, and 0.6 mW under the loading resistance of 20  $\text{M}\Omega$ , 2, and 1  $\text{k}\Omega$ , respectively. It is needed to note that the swing angle of bifilar-pendulum in the simulated wave height is lower than the rotation angle of seesaw simulation test. Therefore, when the vessel with incorporated BCHNG modules operate at the real ocean waves, the BCHNG module will achieve a higher power density. Furthermore, under the driving of simulated water wave, the charge curves of three kinds of generators and BCHNG module are studied by two 100  $\mu\text{F}$  capacitors in series (Figure 4e). It is clear that the BCHNG module integrating three generators has a faster charging capacity rate. Although the loaded impedance of the three generators is not the same, compared with that of one generator, the simple superposition of three generators can still effectively improve the collection efficiency of water wave energy. The energy conversion efficiency of BCHNG module can be further enhanced by developing a suitable power management circuits in the future. As displayed in Figure 4f–k, open-circuit voltage of M-TENG, PENG, and EMG are 650, 11, and 0.65 V and the corresponding short-circuit current is 150  $\mu\text{A}$ , 6, and 2.2 mA, respectively. In addition, the relational transferred charges of M-TENG and PENG are shown in Figure S18, Supporting Information, and we can easily find the transferred charges of 1.08 and 5.0  $\mu\text{C}$  are realized.

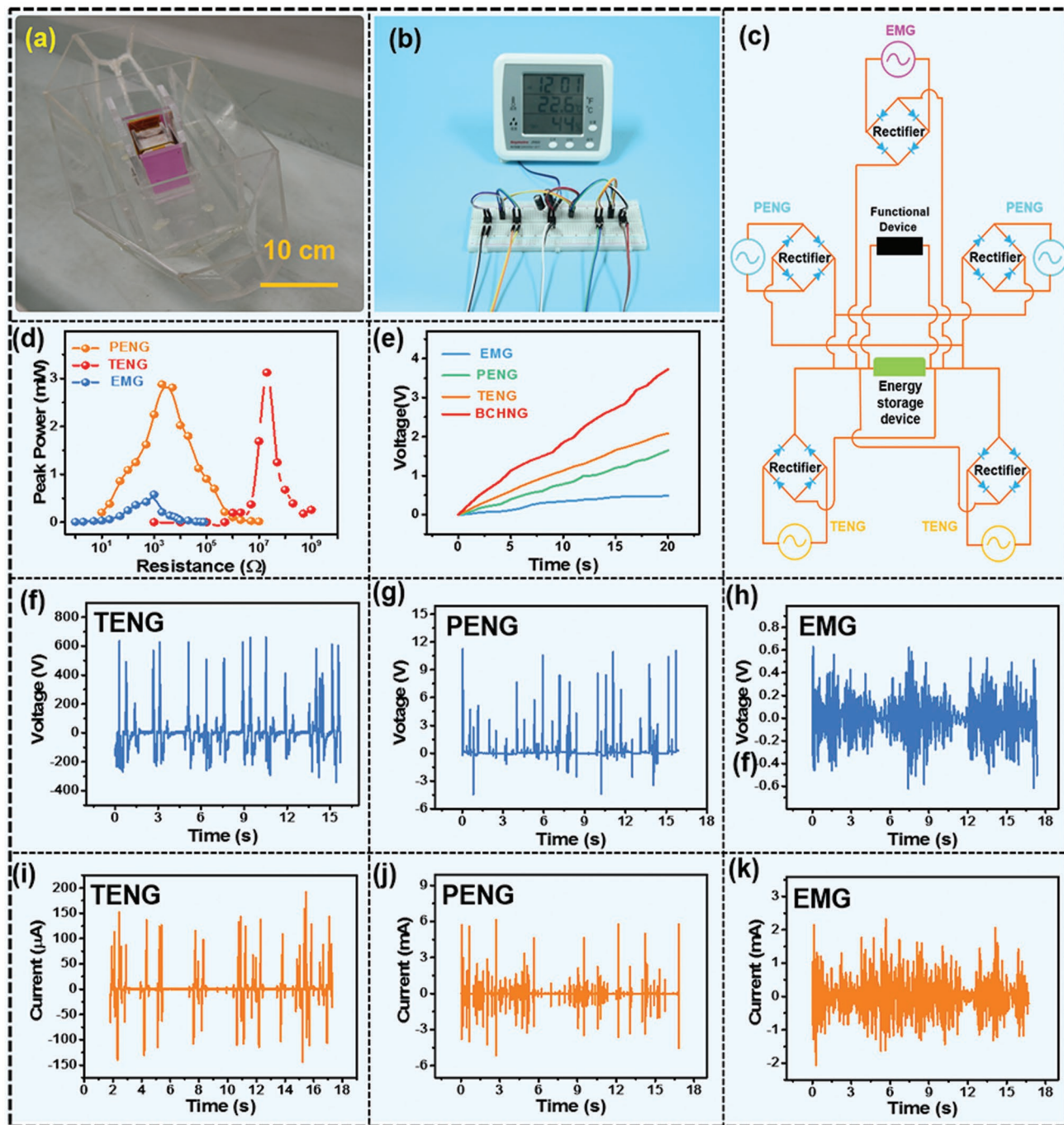


**Figure 4.** Output performance and application of the boat with incorporated BCHNG modules in water wave. a) The photo of boat with incorporated BCHNG modules in water tank. b) Demonstration of the boat incorporated with the BCHNG module as a power source to drive a hygrothermograph. c) The corresponding circuit diagram of BCHNG module to driving functional device. d) The corresponding peak-power–resistance profiles of BCHNG module with three kinds of generators. e) The charge curve of three kinds of generators and BCHNG module. Open-circuit voltage of BCHNG with f) M-TENG, g) PENG, and h) EMG in the simulated water waves. Short-circuit current of BCHNG with i) M-TENG, j) PENG, and k) EMG in the simulated water waves.

### 3. Conclusions

In summary, BCHNG modules incorporated in a vessel is provided to harvest ocean-wave energy. Because the bifilar-pendulum cone is fabricated by using the heavy

characteristics of PENG and the coil of EMG as the PTO and the light-weight characteristics of TENG is used to balance the weight of bifilar-pendulum cone, the captured power of BCHNG modules with water wave energy can be significantly increased and a floating wave energy collection device with the

advantages of simple installation and maintenance can be realized. The BCHNG module can harvest the kinetic energy and gravitational potential energy of ocean-wave at the same time, which is based on the swing of bifilar-pendulum. In addition, benefiting from the reasonable utilization of space by coupling PENG and EMG, the BCHNG module obtains an excellent output performance with a power density of  $358.5 \text{ W m}^{-3}$ , which is increased by one or two orders of magnitude compared to previous related work. Meanwhile, the output performance of the BCHNG module can be further improved by optimizing parameters such as the number of units in M-TENG, the number of coils in EMG, the magnetic field strength of the magnet, and the thickness of ceramic plates in PENG. More importantly, thanks to the advantages of vessel platform, the module can obtain higher output performance and good adaptive capacity in real marine environment without complex isolation protection. Finally, the vessel platform provides enough space for the BCHNG modules to integrate with other technology modules, such as, desalination and marine sensor to achieve a self-powered marine resource development and marine monitoring in situ. In a word, this work provides a new and effective method to harvest the ocean-wave energy.

#### 4. Experimental Section

**Fabrication of the M-TENG:** First, a  $42 \text{ cm} \times 5 \text{ cm} \times 30 \text{ }\mu\text{m}$  Kapton film with evenly spaced intervals of  $7 \text{ cm}$  was applied as the substrate for M-TENG, on which, a foam with  $50 \text{ }\mu\text{m}$  ( $7 \text{ cm} \times 5 \text{ cm} \times 50 \text{ }\mu\text{m}$ ) to achieve a better contact was attached on each interval. Then, a copper foil ( $4.5 \text{ cm} \times 6 \text{ cm}$ ) was adhered on each foam to form one electrode. For another electrode, a FEP film ( $4.5 \text{ cm} \times 6 \text{ cm} \times 30 \text{ }\mu\text{m}$ ) as dielectric layer was stuck on another copper foil. The FEP, copper, and foam were pasted on the alternate interval of the Kapton. Then the entire Kapton was bent to a zigzag structure to achieve M-TENG.

**Fabrication of the PENG:** The corresponding structure of PENG is displayed in Figure S1b, Supporting Information; a copper electrode with the size of  $5 \text{ cm} \times 7 \text{ cm} \times 0.5 \text{ mm}$  was coated with a  $4.8 \text{ cm} \times 5.0 \text{ cm} \times 0.2 \text{ mm}$  PZT piezoceramics on both sides and kept the same polarity of the PZT connected to the copper electrode. In addition, the other surface of the two PZTs was coated with a silver electrode of about  $0.1 \text{ mm}$ .

**Fabrication of the EMG:** At first, enameled wire with a diameter of  $0.2 \text{ mm}$  with about 50 000 loops was wound around a copper wedge-shape pendulum cone of bifilar-pendulum to be the coil of EMG. A pair of wedge-shaped magnet on the opposite sides was used to make the coil cut the magnetic induction line and generate electric energy.

**Fabrication of the BCHNG Module:** The BCHNG modules consisted of an EMG, two PENGs, and two M-TENGs as shown in Figure 1c. Herein, the wedge-shaped pendulum cone was used to increase the contact area of M-TENG. Next, a square acrylic (size:  $2 \text{ cm} \times 1 \text{ cm} \times 1 \text{ cm}$ ) with a hole in the center of side (diameter:  $6 \text{ mm}$ ) was attached on the top of bifilar-pendulum cone and the bifilar-pendulum cone is fixed to the bracket by using a fishing line (diameter:  $1 \text{ mm}$ , length:  $13 \text{ cm}$ ). Finally, the effective volume of BCHNG module was composed of a cuboid with a volume of about  $400 \text{ cm}^3$  ( $10 \text{ cm} \times 6 \text{ cm} \times 6.7 \text{ cm}$ ).

**Fabrication of the Boat:** The boat with the size of  $50 \text{ cm} \times 20 \text{ cm} \times 30 \text{ cm}$  was fabricated with acrylic sheet. To ensure the lateral stability of boat, a pair of acrylic blocks with  $20 \text{ cm} \times 10 \text{ cm}$  was symmetrically added on both sides of the hull as a fin stabilizer to eliminate the influence of transverse water waves in the ship's motion in direction of water wave propagation

**Electrical Measurement of the BCHNG module:** For the electric output measurement of the modules, a linear motor (TSMV120-1S) and a

seesaw were utilized to drive the BCHNG, and a  $2.7 \text{ m} \times 0.7 \text{ m} \times 0.7 \text{ m}$  of water tank was used to simulate the wave. The programmable electrometer (Keithley model 6514) was applied to test the transferred charges and short-circuit current. The mixed domain oscilloscope (MDO3024) was utilized to test the open-circuit voltage. A potentiostat (Biologic, VMP3) was utilized to test the voltage of the capacitor in charging capacitor test.

#### Supporting Information

Supporting Information is available from the Wiley Online Library or from the author.

#### Acknowledgements

C.Z., W.Y., and B.Z. contributed equally to this work. Research was supported by the National Key R & D Project from Minister of Science and Technology (2016YFA0202704), Beijing Municipal Science & Technology Commission (Z171100000317001, Z171100002017017, and Y3993113DF), The Key Research Program of Frontier Sciences, Chinese Academy of Sciences (ZDBS-LY-DQC025), National Natural Science Foundation of China (Grant Nos. 61774016, 21773009, 5151101243, and 51561145021), and the Fundamental Research Funds for the Central Universities (E1E46802). The authors also thank Haining Yu for this work.

#### Conflict of Interest

The authors declare no conflict of interest.

#### Data Availability Statement

Research data are not shared.

#### Keywords

bifilar-pendulum, piezoelectric nanogenerators, triboelectric nanogenerators, wave energy harvesting

Received: November 25, 2021

Revised: January 10, 2022

Published online: January 27, 2022

- [1] D. Mollison, O. P. Buneman, S. H. Salter, *Nature* **1976**, 263, 223.
- [2] C. Rodrigues, D. Nunes, D. Clemente, N. Mathias, J. M. Correia, P. Rosa-Santos, F. Taveira-Pinto, T. Morais, A. Pereira, J. Ventura, *Energy Environ. Sci.* **2020**, 13, 2657.
- [3] Y. Zi, H. Guo, Z. Wen, M. H. Yeh, C. Hu, Z. L. Wang, *ACS Nano* **2016**, 10, 4797.
- [4] W. Li, K. T. Chau, C. H. Lee, T. W. Ching, M. Chen, J. Z. Jiang, *Renewable Energy* **2017**, 105, 199.
- [5] S. Doyle, G. A. Aggidis, *Renewable Sustainable Energy Rev.* **2019**, 107, 75.
- [6] F. Chen, D. Duan, Q. Han, X. Yang, F. Zhao, *Energy Convers. Manage.* **2019**, 182, 191.
- [7] S. An, H. S. Jo, G. Li, E. Samuel, S. S. Yoon, A. L. Yarin, *Adv. Funct. Mater.* **2020**, 30, 2001150.
- [8] X. Liang, T. Jiang, G. Liu, Y. Feng, C. Zhang, Z. L. Wang, *Energy Environ. Sci.* **2020**, 13, 277.

- [9] E. Stokstad, *Science* **2016**, 352, 637.
- [10] S. Kazemi, M. Nili-Ahmadabadi, M. R. Tavakoli, R. Tikani, *Renewable Energy* **2021**, 179, 528.
- [11] M. Penalba, J. Ringwood, *Energies* **2016**, 9, 506.
- [12] L. Zhou, D. Liu, J. Wang, Z. L. Wang, *Friction* **2020**, 8, 481.
- [13] L. Chen, C. Chen, L. Jin, H. Guo, A. C. Wang, F. Ning, Q. Xu, Z. Du, F. Wang, Z. L. Wang, *Energy Environ. Sci.* **2021**, 14, 955.
- [14] C. Zhang, Y. Liu, B. Zhang, O. Yang, W. Yuan, L. He, X. Wei, J. Wang, Z. L. Wang, *ACS Energy Lett.* **2021**, 6, 1490.
- [15] Y. Zhang, Z. Huo, X. Wang, X. Han, W. Wu, B. Wan, H. Wang, J. Zhai, J. Tao, C. Pan, Z. L. Wang, *Nat. Commun.* **2020**, 11, 5629.
- [16] H. Guo, X. Pu, J. Chen, Y. Meng, M. H. Yeh, G. Liu, Q. Tang, B. Chen, D. Liu, S. Qi, C. Wu, C. Hu, J. Wang, Z. L. Wang, *Sci. Rob.* **2018**, 3, eaat2516.
- [17] C. Li, D. Liu, C. Xu, Z. Wang, S. Shu, Z. Sun, W. Tang, Z. L. Wang, *Nat. Commun.* **2021**, 12, 2950.
- [18] H. Guo, J. Chen, L. Wang, A. C. Wang, Y. Li, C. An, J. He, C. Hu, V. Hsiao, Z. L. Wang, *Nat. Sustain.* **2021**, 4, 147.
- [19] C. Zhang, L. Liu, L. Zhou, X. Yin, X. Wei, Y. Hu, Y. Liu, S. Chen, J. Wang, Z. L. Wang, *ACS Nano* **2020**, 14, 7092.
- [20] Z. Zhou, K. Chen, X. Li, S. Zhang, Y. Wu, Y. Zhou, K. Meng, C. Sun, Q. He, W. Fan, E. Fan, Z. Lin, X. Tan, W. Deng, J. Yang, J. Chen, *Nat. Electron.* **2020**, 3, 571.
- [21] Y. Shi, F. Wang, J. Tian, S. Li, E. Fu, J. Nie, R. Lei, Y. Ding, X. Chen, Z. L. Wang, *Sci. Adv.* **2021**, 7, eabe2943.
- [22] J. Yu, G. Gao, J. Huang, X. Yang, J. Han, H. Zhang, Y. Chen, C. Zhao, Q. Sun, Z. L. Wang, *Nat. Commun.* **2021**, 12, 1581.
- [23] G. Chen, Y. Li, M. Bick, J. Chen, *Chem. Rev.* **2020**, 120, 3668.
- [24] N. Zhang, F. Huang, S. Zhao, X. Lv, Y. Zhou, S. Xiang, S. Xu, Y. Li, G. Chen, C. Tao, Y. Nie, J. Chen, X. Fan, *Matter* **2020**, 2, 1260.
- [25] J. Chen, Y. Huang, N. Zhang, H. Zou, R. Liu, C. Tao, X. Fan, Z. L. Wang, *Nat. Energy* **2016**, 1, 16138.
- [26] C. Zhang, L. Zhou, P. Cheng, D. Liu, C. Zhang, X. Li, S. Li, J. Wang, Z. L. Wang, *Adv. Energy Mater.* **2021**, 11, 2003616.
- [27] P. Cheng, H. Guo, Z. Wen, C. Zhang, X. Yin, X. Li, D. Liu, W. Song, X. Sun, J. Wang, Z. L. Wang, *Nano Energy* **2019**, 57, 432.
- [28] X. Liang, T. Jiang, Y. Feng, P. Lu, J. An, Z. L. Wang, *Adv. Energy Mater.* **2020**, 10, 20026123.
- [29] X. Wei, Z. Zhao, C. Zhang, W. Yuan, Z. Wu, J. Wang, Z. L. Wang, *ACS Nano* **2021**, 15, 13200.
- [30] J. Chen, J. Yang, Z. Li, X. Fan, Y. Zi, Q. Jing, H. Guo, Z. Wen, K. C. Pradel, S. Niu, Z. L. Wang, *ACS Nano* **2015**, 9, 3324.
- [31] G. Zhu, Y. Su, P. Bai, J. Chen, Q. Jing, W. Yang, Z. L. Wang, *ACS Nano* **2014**, 8, 6031.
- [32] Y. Su, X. Wen, G. Zhu, J. Yang, J. Chen, P. Bai, Z. Wu, Y. Jiang, Z. L. Wang, *Nano Energy* **2014**, 9, 186.
- [33] Q. Jing, G. Zhu, P. Bai, Y. Xie, J. Chen, R. Han, Z. L. Wang, *ACS Nano* **2014**, 8, 3836.
- [34] L. Feng, G. Liu, H. Guo, Q. Tang, X. Pu, J. Chen, X. Wang, Y. Xi, C. Hu, *Nano Energy* **2018**, 47, 217.
- [35] S. Zhang, M. Xu, C. Zhang, Y. Wang, H. Zou, X. He, Z. Wang, Z. L. Wang, *Nano Energy* **2018**, 48, 421.
- [36] J. Wang, L. Pan, H. Guo, B. Zhang, R. Zhang, Z. Wu, C. Wu, L. Yang, R. Liao, Z. L. Wang, *Adv. Energy Mater.* **2019**, 9, 1802892.
- [37] Z. Wu, H. Guo, W. Ding, Y. Wang, L. Zhang, Z. L. Wang, *ACS Nano* **2019**, 13, 2349.
- [38] C. Zhang, L. He, L. Zhou, O. Yang, W. Yuan, X. Wei, Y. Liu, L. Lu, J. Wang, Z. L. Wang, *Joule* **2021**, 5, 1613.
- [39] H. Li, L. Su, S. Yang, K. Cao, F. Pan, G. Zhu, Z. L. Wang, *Adv. Funct. Mater.* **2015**, 25, 5691.
- [40] J. Wang, S. Li, F. Yi, Y. Zi, J. Lin, X. Wang, Y. Xu, Z. L. Wang, *Nat. Commun.* **2016**, 7, 12744.
- [41] Y. Feng, X. Liang, J. An, T. Jiang, Z. L. Wang, *Nano Energy* **2020**, 81, 105625.
- [42] H. Wang, L. Xu, Y. Bai, Z. L. Wang, *Nat. Commun.* **2020**, 11, 4203.
- [43] C. Hao, J. He, C. Zhai, W. Jia, L. Song, J. Cho, X. Chou, C. Xue, *Nano Energy* **2019**, 58, 147.
- [44] W. Liu, W. Liu, Z. Wang, G. Wang, G. Liu, J. Chen, X. Pu, Y. Xi, X. Wang, H. Guo, C. Hu, Z. L. Wang, *Nat. Commun.* **2019**, 10, 1426.
- [45] Y. Li, Z. Zhao, L. Liu, L. Zhou, D. Liu, S. Li, S. Chen, Y. Dai, J. Wang, Z. L. Wang, *Adv. Energy Mater.* **2021**, 15, 2100050.
- [46] S. Wang, Y. Xie, S. Niu, L. Lin, C. Liu, Y. Zhou, Z. L. Wang, *Adv. Mater.* **2014**, 26, 6720.
- [47] H. Hong, X. Yang, H. Cui, D. Zheng, H. Wen, R. Huang, L. Liu, J. Duan, Q. Tang, *Energy Environ. Sci.* **2022**, <https://doi.org/10.1039/d1ee02549j>.
- [48] Z. Yuan, C. Wang, J. Xi, X. Han, J. Li, S. Han, W. Gao, C. Pan, *ACS Energy Lett.* **2021**, 8, 2809.